Heliyon 6 (2020) e05547

Contents lists available at ScienceDirect

Heliyon

journal homepage: www.cell.com/heliyon

Research article

Evaluation of the active contour and topographic watershed segmentation "assessment of the systolic ejection fraction in the left ventricular for medical assistance in 5D short axis cine MRI"

Houneida Sakly [a,*], Mourad Said [b], Moncef Tagina [a]

[a] COSMOS Laboratory, National School of Computer Sciences (ENSI), University of Manouba, Tunisia
[b] Radiology and Medical Imaging Unit, International Center Carthage Medical, Tourist Area "JINEN EL OUEST" 5000 Monastir, Tunisia

ARTICLE INFO

Keywords:
Computer science
Engineering
Cardiology
Medical imaging
Biomedical engineering
Radiology
Clinical research
Contour segmentation
Topographic watershed segmentation
Short-axis 5D cardiac sequences
MRI
Medical decision making

ABSTRACT

A comparative study has been depicted between the contour and topographic watershed segmentation approach for short-axis 5D cardiac sequences with MRI for medical decision. The fifth dimension has been defined as the excitation of pixels based on the gray scale around the myocardium without consideration of the morphological structure of the heart in 3D and fourth dimension (time). Three patients were performed the first is healthy, the second has a genetic disease, and the third had a heart failure syndrome for a dimension ROI = 150mm, average age is 54 years old, and mean of weight = 86 kg. A contouring and watershed segmentation algorithm for a sample of 63 Cine Fiesta MRI sequences for short-axis cuts with Matlab and its in-box toolbox complements was implemented.

For a healthy patient 13.4% tolerance rate for the estimation of the stroke fraction, 6.4% for a patient with genetic disease, 8.7% error rate for a patient with heart failure symptom. The results show that the regurgitation fraction by the contour approach for a patient case with symptom of the presence of a genetic disease is 0.0335% for an aortic valve, 0.248% for a mitral valve, an error rate 0.16% for estimating this parameter for the aortic orifice with the watershed segmentation approach. In return, for a patient with suspected heart failure (stenosis or regurgitation) the regurgitation fraction is estimated by 0% for aortic valve, 1.49 e^{+03}% for a mitral valve, an error rate 11.76% compared to the watershed segmentation approach. The results are validated clinically. The Optimization of the topographic watershed approach with mutual information was simulated for the extraction of measurements (ejection fraction, regurgitation rate) within the left ventricle for three patient types (healthy, genetic pathology and heart failure). The results are considered interesting compared to the clinical assessment.

1. Introduction

The segmentation task of the medical image that offers a large number of distinct loci for interaction that can act on a deep level for diagnostic assistance. Image segmentation based in various models and partial differential equations are promoter in view of their flexibility and computing performance. Segmentation models can be classified into contour-based models [1, 2, 3] or on the classification of regions [4, 5, 6]. Contour methods extract local features as well as first and second order derivatives of the image. The major drawback is the noise control during image processing. The variational problem offers a solution based on chunks with smooth boundaries. During iterations of numerical computation, the setting is crucial and topological changes are not allowed. Selective segmentation models are considered most suitable for applications, such as surgical simulation, medical diagnosis, object tracking, etc., to ensure the finality of experts to extract objects of interest in the image object of prognosis [7]. Gout et al. [8] introduced use a set of landmarks on the contour of interest for the geodesic active contour model based on geometry constraint. Later Badshah et Chen [9] proposed to improve the results by combining the term region with the region information in order to make the model more robust, especially for noisy images. These two level set functions perform two tasks simultaneously to describe a new variational model [10]. The object of segmentation is used to track the boundaries and the other focuses on the region of interest which is close to geometric constraints. The average channel image, which can extract textural and inhomogeneous objects introduces

* Corresponding author.
E-mail address: houneida.sakly@esiee.fr (H. Sakly).

https://doi.org/10.1016/j.heliyon.2020.e05547
Received 19 October 2019; Received in revised form 3 October 2020; Accepted 16 November 2020

Table 1. Recent work and contribution.

Approach for cardiac imaging	Dimension	Conditions of acquisition
Contour Segmentation [19, 20]	4D (3D + t)	Short axis sequences
Region Segmentation [21, 22]	3D	
Fully automatic segmentation [23, 24]	4D (3D + t)	
Watershed Segmentation [25, 26]	3D +4D	left atrial surface + Short axis sequences
Our purpose: Contour segmentation + watershed segmentation	5D (3D + Time + Blood flow) [27, 28,29]	Short axis cine Fiesta and its study of flow in apnea

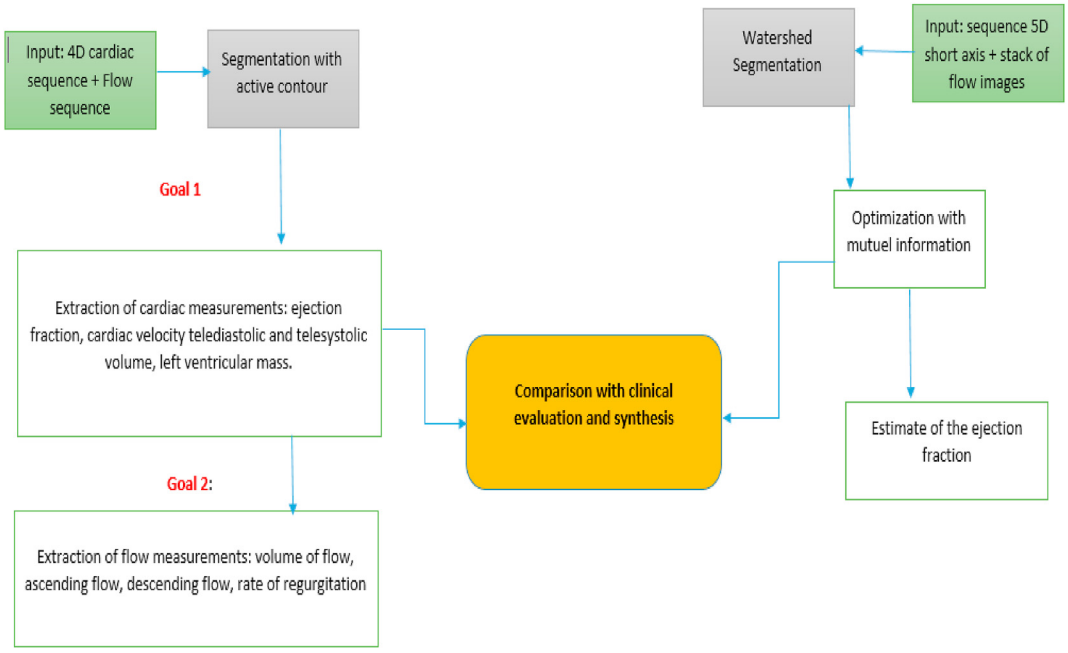

Figure 1. Goals and contribution.

the selective segmentation model [11, 12]. Several research projects have focused on watershed segmentation. Image decision making is often deduced from the first segment the image (ie, gathering neighboring pixels into homogeneous regions) and then a classification step based on the supervised region. In such a process that uses watershed approach [13], the type of the segmentation stage is crucial for the final graded result. The watershed algorithm dynamically combines nodes into homogeneous network segments regarding their topological relationships and detection states. These groups of distributed data streams allow manipulation in space instead of individual nodes in order to realize network segments as programming abstractions describing various query processes to be executed [14]. This method proves its effectiveness in the field of medical imaging segmentation in research work [15, 16, 17, 18]. In this paper, our main objective is to make a comparative study between these two approaches, their impact in the diagnosis for the identification of heart and valvular diseases, to value the results obtained in the context of medical prognosis.

2. Contribution

The validation of our approach for the design of short-axis 5D cuts requires clinical validation through the segmentation phase. This step allows the experts to deduce a set of measurements for left ventricular analysis (tele-diastolic volume, tele-systolic volume, systolic ejection volume, indexed tele-diastolic volume, indexed tele-systolic volume, cardiac output, systolic ejection fraction, cardiac index, maximal filling rate, left ventricular mass, cardiac index, flow compensation ...), as well as the maximum and minimum velocity rate for the study of valvulopathies. Indeed, the segmentation approach adopted by the clinical environment is the endocardial and epicardial contour method in order to extract these dies. At this point, the physician adjusts the perimeter of the myocardial muscle by pointing to the contour so that the "Report-Card" diagnostic platform filed by "General Electric Healthcare" connects these points to obtain the final shape of the contour. This technique suffers from several deficiencies that can affect the accuracy of the cardiac parameters and subsequently the medical inference.

Several previous works have focused on 2D and 3D dimension-based cardiac imaging segmentation approaches such as segmentation by contour, region and watershed. The size and type of slices during examination

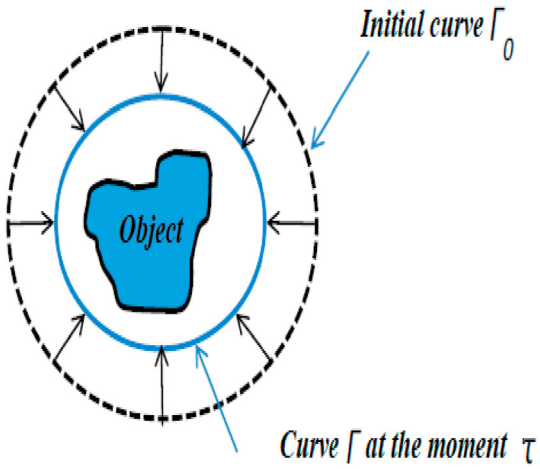

Figure 2. Illustration of the CA evolution process towards the contours of the object of interest [21].

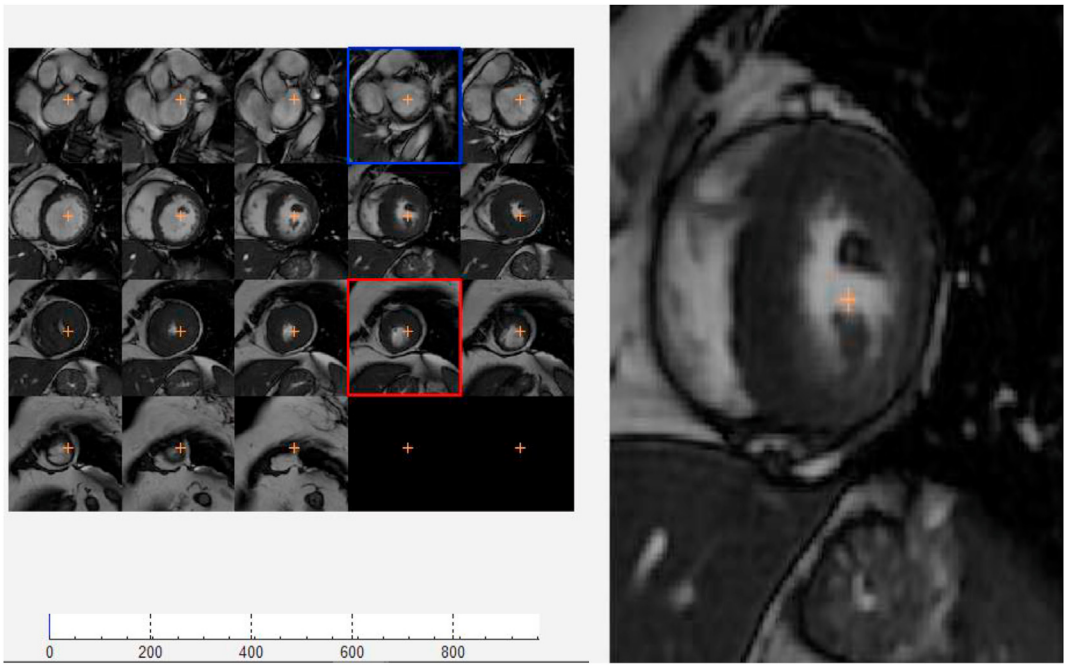

Figure 3. (a) basal slice (blue) selection of myocardium (b) apical epicardial selection (red) for segmentation of 3 patients.

have an impact on extracted measurements and their precision for decision making. for purpose it is to develop a fifth dimension of flow which consists in extracting new measurements for medical diagnosis. A comparative study has been described to evaluate the precision of the fraction measurement systolic ejection by adopting the approach of segmentation by contour and by watershed. Table.1 presents a summary of recent work based on segmentation approach comparing in our contribution.

Following this context, our main contribution consists to re-estimate some parameters and extract new measures for the flow study compared to the clinical assessment. The work seeks to is to estimate the fraction of systolic ejection with the watershed approach to deduce the contribution of our strategy and to make a synthesis for what is most suitable for the medical diagnosis. Figure 1 summarizes this vision as well as the valuation of the objectives of each task.

3. Methods and materiels

To apply our methodology, we chose three patients: the first is healthy, the second has a genetic disease, and the third had a heart failure syndrome for a dimension ROI = 150mm. The first case aged 53 had the following coordinates: 76.4 kg weight, 155 cm height, area of Body Area (ASC) 1.8 m^2. Our study is articulated around 360 cuts of type 2 short-Axis Cine-MRI with slice position = -64.691.

The third 59-year-old case had the following coordinates: 78 kg of weight, with 400 cuts of type Short-axis cine-MRI with slice position = -96.737. The last patient had 54-year-old case and the following coordinates: 106 kg weight, 172 cm height, body Surface Area (ASC) 2.2 m^2. The 300 cuts are of type short-axis cine-MRI with slice position = -104.81.

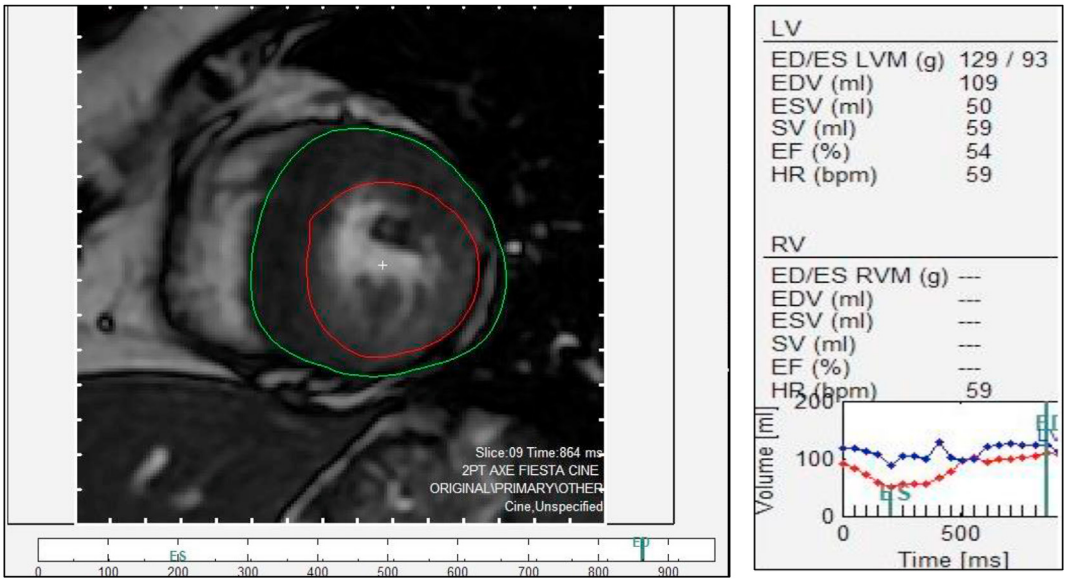

Figure 4. Segmentation of the left ventricle and extraction of cardiac measurements for a healthy patient.

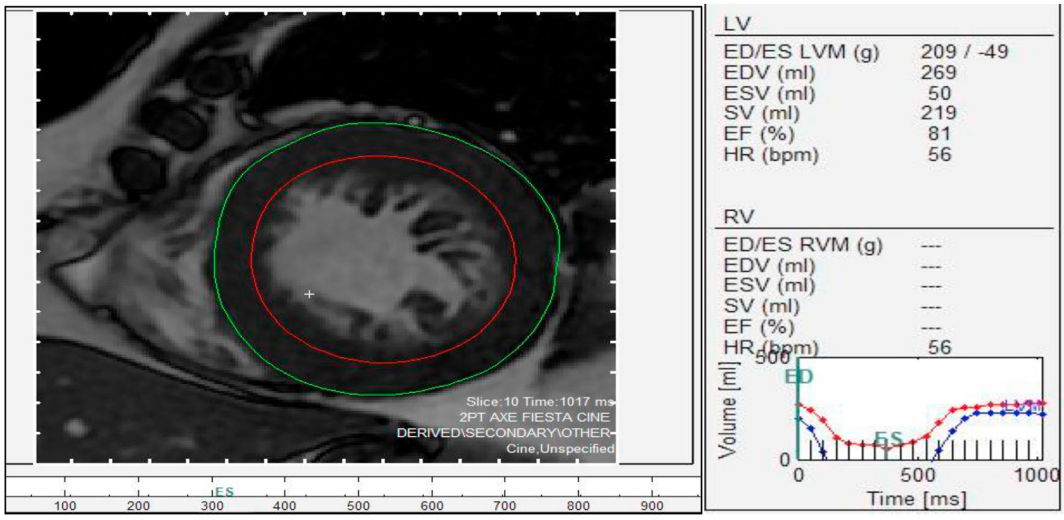

Figure 5. Segmentation of the left ventricle and extraction of cardiac measurements for the second patient with presence of genetic abnormality.

We used as tools to implement the contour segmentation approach and watershed: MATLAB, the MEDVISO platform with the Platform OPENGL., MIPAR V1.5.6 for the estimation and evaluation of cardiac measurements for the study of sequences of flow, we generated the stacks with the MRIcros project and the Batch Processor toolbox for a 38-year-old patient, 180cm tall and moderate obese with 101kg and ASC = 202cm^2. These flow studies are depicted as QFlow sequences with slice position = -115.75 in 360 acquired in real time. Informed consent was obtained from all patients for our experiments within the International Center Carthage Medical in Tunisia.

4. Mathematical concepts, experiments and results

In this section, we will implement the contour segmentation approach for left ventricle analysis. This study will be divided into two parts: the extraction of a measurement set for each patient and comparing it with the clinical assessment, and in the second stage it is to estimate indices for the aid to the identification of valvulopathies.

4.1. Active contour segmentation in the left ventricular: estimation and extraction of cardiac measurements

4.1.1. Mathematical concept

An active contour (CA) is a curve that evolves from an initial shape to the boundaries of the object of interest. The CA technique has become very popular and is widely used in image segmentation. The main objective of this technique is to segment an object by iteratively deforming a contour until it reaches the contours of the object by minimizing an energy calculated from different criteria. During this minimization process, the points of the curve will move so that the curve at the next iteration has a lower energy; and the CA thus evolves until it reaches the boundaries of the desired object.

Figure 2 illustrates the process of converging the CA from its initial state to the boundaries of the object of interest. An operator, prior knowledge or other processing on the first image must provide the initial state. Let us denote I an image defined on a domain Ω and I (x) the intensity of the pixel x such that x Jukcy Ω. We use in our work the level

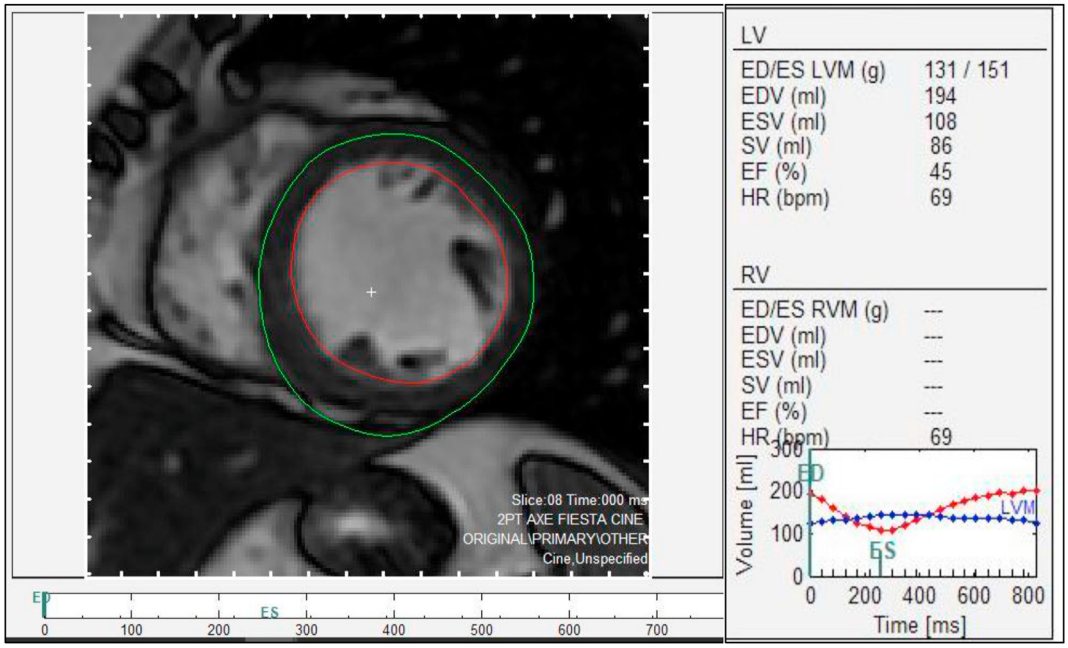

Figure 6. Segmentation of the left ventricle and extraction of cardiac measurements for the third patient with heart failure syndrome.

Figure 7. Patient with suspicion of presence of genetic disease (a) correspondence between hunting chamber sequences and their flow study, (b) blood flow compensation.

set method which considers the evolutionary curve as the zero level of a surface [30, 31]. The distortion of the surface induces a deformation on the shape of the curve. This process stimulates the evolution of the turnover and, eventually, the segmentation of the object of interest. Let C be a firm contour representing the zero level of these sets of levels of a signed distance function ϕ, (i.e., $C = \{x \mid \phi(x) = 0\}$). The purpose of this process is to implicitly evolve the contour C such that the convergence ϕ <0, (the inside of C) and ϕ> 0 (the outside of C) respectively represent the object of interest and the bottom. In the formulation of sets of levels, a Heaviside function is used to specify the interior and exterior of C [32]. The following approximation of the Heaviside function Ꮋ ϕ (x) specifies the interior of C:ϕ(x)

$$H\Phi(x) = \begin{cases} \Phi(x) > \varepsilon \\ \frac{1}{2}\left(1 + \frac{\Phi}{\varepsilon} + \frac{1}{\pi}\cdot\sin\cdot\frac{\pi\cdot\Phi(x)}{\varepsilon}\right), \\ \text{ailleurs} \end{cases} \tag{1}$$

Similarly, the outside of C is specified by ((1- Ꮋ ϕ (x)) The energy is calculated only on a narrow band around C in order to decrease the complexity of the calculation of the standard method of sets of levels [33]. This area around C is specified by the derivative of Ꮋ ϕ (x) and is defined by the Dirac delta function δϕ (x) as follows:

$$\delta\Phi(x) = \begin{cases} 1 \quad \Phi(x) = 0 \\ 0 \quad |\Phi(x)| < \varepsilon \\ \frac{1}{2\varepsilon}\cdot\left(1 + \cos\frac{\pi\,\Phi(x)}{\varepsilon}\right), \\ \text{ailleurs} \end{cases} \tag{2}$$

4.1.2. Contour segmentation for short-axis cuts

In this section, we use this mathematical concept to implement an algorithmic approach to active contour segmentation to evaluate and analyze the left ventricle. We start our case study by a healthy patient and a medical conclusion with no cardiac abnormalities as well as a second patient

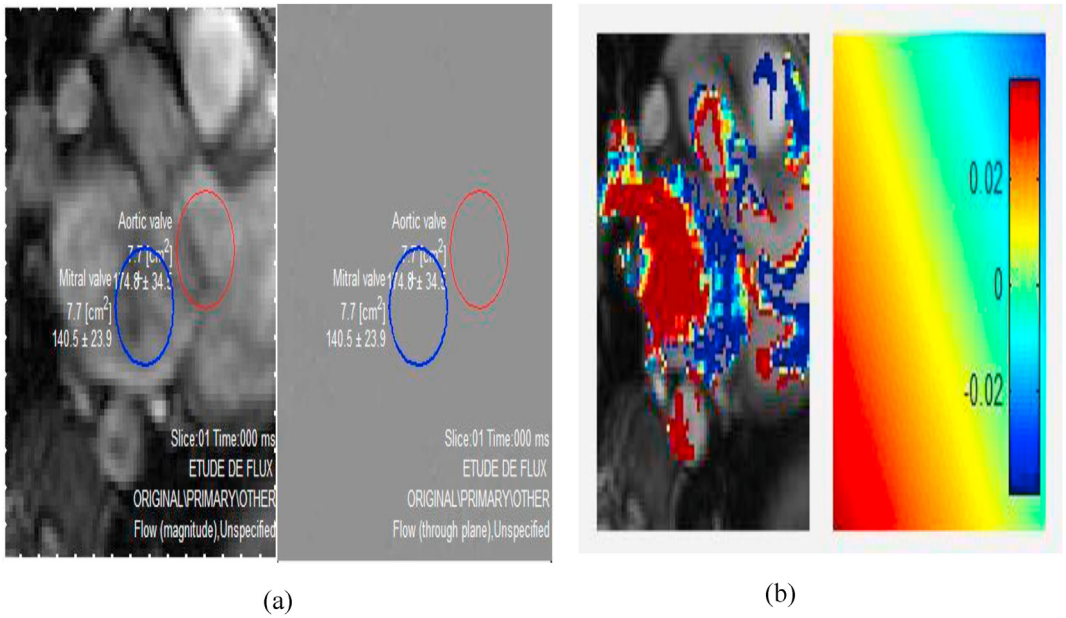

Figure 8. Patient with suspected heart failure (a) correspondence between hunting chamber sequences and their flow study, (b) blood flow compensation.

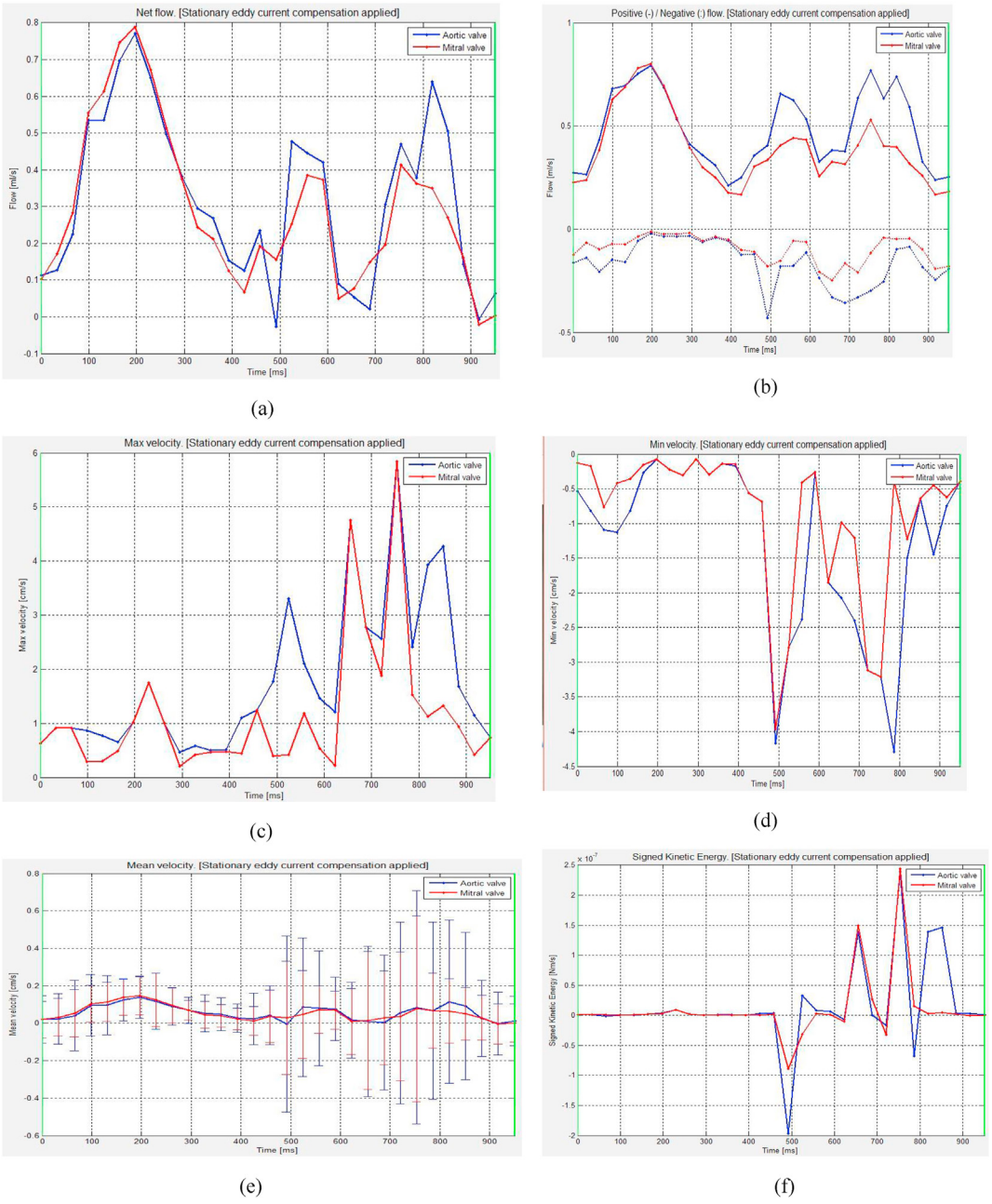

Figure 9. Flow study for a patient with genetic pathology syndrome (a) blood flow simulation, (b) negative and positive flow simulation, (c) maximum blood flow velocity, (d) minimal blood flow velocity, (e) Average blood velocity, (f) Kinetic energy.

with a confirmed genetic disease and a third case with heart failure syndrome are shown respectively in Figure 3, Figure 4.Figure 5 and Figure 6.

The parameters that are deduced as a result for the first patient: myocardial mass in the diastolic ejection = 129g, myocardial mass in the systolic ejection = 93g, a systolic ejection volume = 50 ml, a diastolic ejection volume = 109 ml, systolic volume = 59 ml, systolic ejection fraction = 54% and cardiac output 59 bpm in Figure 4. We also obtained a simulation of systolic ejection volume as a function of time with maximum value 100 ml as well as a representation of the diastolic ejection volume with maximum value about 120 ml.

The parameters that are deduced as a result for a second patient carrying a genetic disease: myocardial mass in the diastolic ejection = 209 g, myocardial mass in the systolic ejection = -49 g, a volume of systolic ejection = 50 ml, a diastolic ejection volume = 269 ml, systolic volume = 219 ml, a systolic ejection fraction = 81% and cardiac output 56 bpm in Figure 5. We also obtained a simulation of systolic ejection volume as a function of time with a maximum value of about 485 ml as well as a representation of the diastolic ejection volume with a maximum value of about 250 ml.

4.1.3. Active contour segmentation for the flow study

In this section, we will exploit the 2D blood flow sequences for the study of valvulopathies. In this case there are two types of valve abnormalities: stenosis and regurgitation. Our case study is limited for the analysis of mitral valve and aortic valve performance in the left part of the heart. The essential signs of mitral stenosis are thickening of valves, the restrictive aspect of their diastolic opening, and dilation of the left atrium and left auricle, whereas aortic valve stenosis is an obstacle hindering the ejection of the blood into systole and resulting in a pressure gradient between the LV and the aorta due to the reduction of the valve opening area. However, the mitral leak corresponds to a reflux of blood from the LV to the LA in systole due to a defect of continence of the mitral

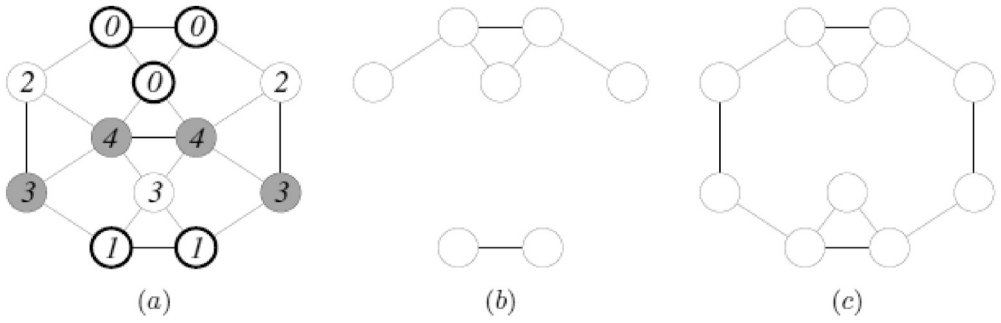

(A)

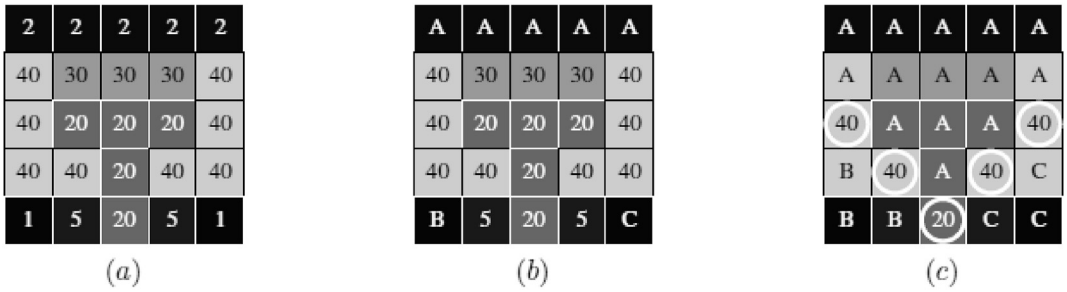

(B)

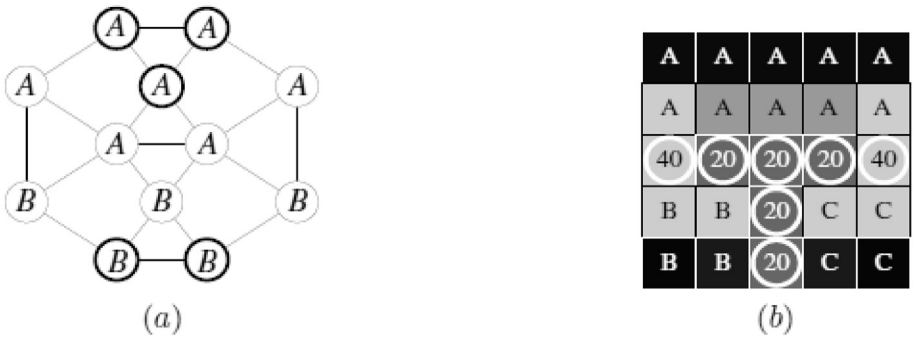

(C)

Figure 10. (A) Graph with valued vertices, lower sections and minima: (a): A graph whose vertices are valued by a function F, vertices which belong to minima of F are surrounded in bold; (b): lower section from F to level 3; (c): lower section from F to level 4; (B) Example of watershed by flooding an image. The presented images are equipped with 4-adjacency. (a): An image F; (b): the minima of F are labeled A, B and C; (c) watersheds (obtained by flooded watershed) are labeled according to the associated minimum F; the corresponding flood EPL consists of unlabeled points (C) Topographic watershed. (a): Amusement basins associated with function F in Fig A. a. The basin of attraction of the minimum of F composed of three (respectively two) vertices is labeled A (or B), (b): The basins of attraction of the function of Fig B equipped with the 4-adjacency [29].

Table 2. Summary of the properties checked by the different watersheds. In the table, S (respectively NS and NA) means satisfied (or does not meet, and does not apply).

Watershed Approach	P1	P2	P3	P4	P5
By Flood	S	NS	NS	?	NS
Topographic	NS	**S**	**S**	**S**	NS
Inter-pixel	NS	S	S	NS	NS
Topological	S	NS	S	NS	NS

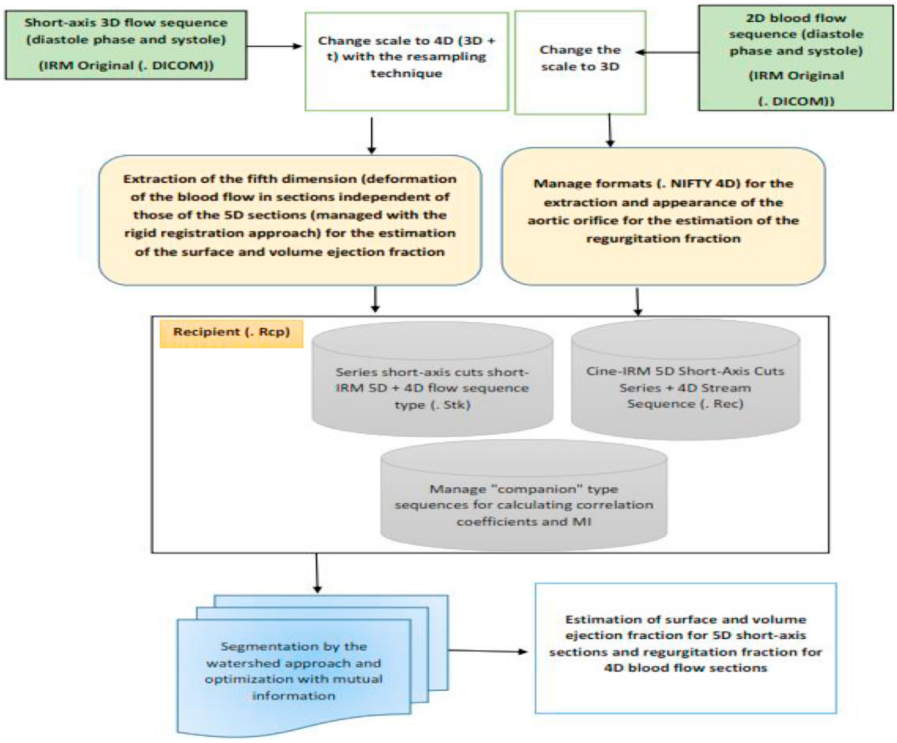

Figure 11. Mode of transformation of medical images and Segmentation procedure.

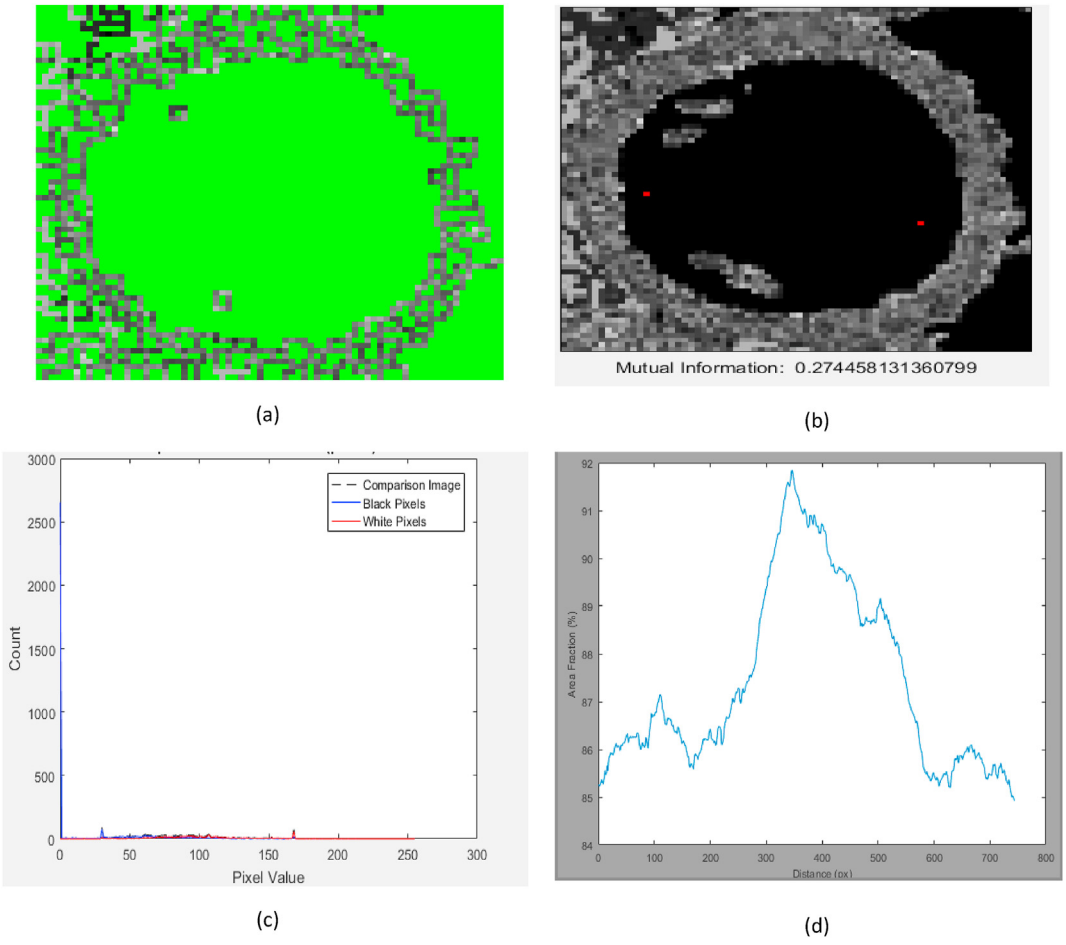

Figure 12. Patient 1: (a) watershed segmentation, (b) calculates the mutual information coefficient, (c) comparison between the original image and the segmented image, (d) estimation of the surface ejection fraction.

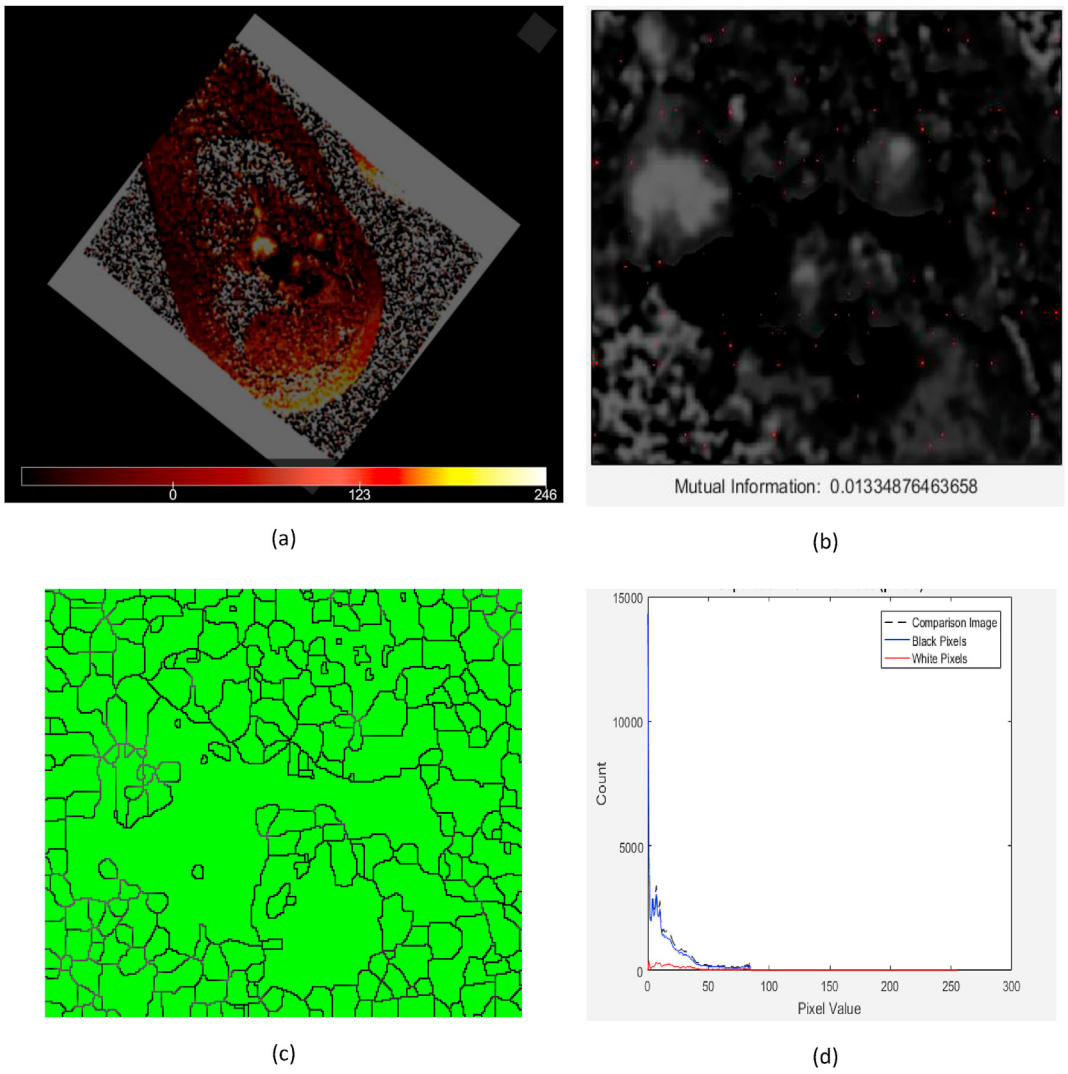

Figure 13. Patient 1: (a) Stack of 4D blood flow, (b) Mutual information coefficient estimation, (c) watershed segmentation, (d) comparison between blood flow sequence and segmented sequence.

valve. On désigne par L'insuffisance aortique correspond au reflux de sang de l'aorte vers le ventricule gauche en diastole en raison d'un défaut de continence de la valve aortique [34].

We selected from our database two patients: the first has a syndrome of genetic disease and the second has a risk of having a heart failure that can be a stenosis or regurgitation. Simulation of aortic and mitral flow as well as maximum and minimum velocity with kinetic energy in a region of interest segmented by the contour approach. The phase of correspondence between the magnitude image (hunting chamber) and the phase image (the study of the blood flow) which consists of identifying the place of the valves in the heart to quantify the compensation of the flow in the selected zone in (Figure 7, Figure 8) and a case of a patient with genetic pathology syndrome described in Figure 9).

In this section, we selected 3 patients (healthy, with heart failure syndrome, with to evaluate the active contour segmentation approach for in order to estimate the following cardiac measures: myocardial mass in diastolic ejection, myocardial mass in systolic ejection, systolic ejection volume, diastolic ejection volume, systolic volume, stroke fraction, and cardiac output Simulated systolic ejection volume versus time as well as a representation of the diastolic ejection volume for these three cases.

Subsequently, we proposed to evaluate the left ventricular contractility function, the radial and fractional velocity behavior, the parietal and fractional thickness, and the estimation of the radius of the zone of interest segmented by the segmentation approach bull's eye with seven sectors.

4.2. Segmentation by the topographic watershed approach: optimization with the mutual information technique and estimation of the ejection fraction

4.2.1. Definition and mathematical concept

For its topographic interest, the watershed is a grayscale image perceived as a topographic relief. The gray level of a pixel in the image shows its altitude in the topographic relief, the dark pixels correspond to the valleys and basins of the relief while the light pixels correspond to the hills and ridges.

Mathematical morphology is the basis of segmentation of the watershed approach. A rigorous definition is proposed in terms of topographic distance. Based on this context, the topographic distance is reduced to the geodesic distance and the watershed becomes the skeleton by zone of influence. The algorithms of minimal paths on graph are revisited and make it possible to propose new algorithms of construction of the watershed; some of them are cited in more detail in [35]. Intuitively, a drop of water falling on a topographic relief flows as quickly as possible to a regional minimum in a descending way [36, 37, 38].

The topographic watershed approach consists in considering M with a minimum of F. The basin of attraction (topographical) of M (for F) is the set of points of V from which M is the only minimum of F which can be reached by a path of greater slope for F. The watershed by topographic distance of F is the set of points of V that do not belong to any basin of

Table 3. Advanced measurement extracted with watershed approach.

	Measurements for the aortic orifice for the first patient	Measurements for the aortic orifice for the second patient
Segmented surface	1882 px	3351 px
Surface fraction (regurgitation)	0.19458%	0.39049%
Ration aspect	2.245	2.0335
Convex zone	2997 px	4120 px
Eccentricity	0.89532	0.87073
Equivalent Diameter	48.9514 px	65.3194 px
Feret diameter	86.3134 px	110.3902 px
Number of characteristic	709	1376
First moment of inertia	1074548.5744 px	2462936.7699 px
First Moment of Inertia/Surface	570.961	734.9856
Length-X	86 px	84 px
Length-Y	60 px	80 px
Major axis length	87.3223 px	97.3236 px
Minor axis length	38.8956 px	47.8596 px
Moment of invariance (Omega-1)	6.5924	9.1185
Moment of invariance (Omega-2)	78.6843	132.5951
Moment of invariance (Phi-1)	0.30338	0.21933
Moment of invariance (Phi-2)	0.033823	-0.016292
Orientation	-8.7065	-51.1875
Perimeter	286.115 px	305.706 px
Perimeter/Area	0.15203	0.091228
Roughness	1.5925	1.2295

attraction. Figure 10 mentions the watershed design with topological distance and its characteristics [38].

4.2.2. Classification of watershed approaches: rationale for choosing the watershed approach by topological distance

Based on the synthetic study that was done by Jean COUSTY [38], the watershed approach by topographic distance has been validated in three mathematical properties compared to the watershed (flood, topological, inter-pixel).

The properties that are addressed in this summary in Table 2 are as follows: Let P ⊆ V be a watershed (flood, topographic, inter-pixel, or topological distance) of F and ψ all the associated basins.

1 The set P is a W-thinning of $\overline{M(F)}$;
2 For every M '∈ ψ, for every point p ∈ M′, there exists, in M ′, a path of greater slope from p to M, M being the unique minimum of F included in M';
3 For any pair of attraction basins M′1; M′2 ∈ ψ, the connection value (for F) between M′1 and M′2 is equal to the connection value (for F) between M1 and M2, the two minima of F such that M1 ⊆ M′1 and M2 ⊆ M′2;
4 For every vertex p of P, there exist M1 and M2 two minima distinct from F which can be reached since p by a descending way;
5 For every vertex p of P, there exist M1 and M2 two minima distinct from F which can be reached since p by π_1 = <p, x1, ... xk> π_2 = <p, y1, ... yl > two descending paths such that xi ∈ M′1, i ∈ [1; k], and yi ∈ M′2, i ∈ [1; l]; M′1 ∈ ψ and M′2 ∈ ψ.

None of the watershed definitions discussed so far will check the five properties presented in Table 2. Intuitively, however, it would seem consistent to have a mathematical framework and a definition of watershed that checks this set of properties. Based on the validation of the watershed approach by topographic distance in relation to these 3 mathematical criteria, our choice to implement it is approved by this notion in order to exploit it to estimate the fraction in surface and volume for the cuts of the 4D blood flow and our 5D short axis sequence.

4.2.3. Description of the mutual information strategy

The mutual information strategy consists of measuring the normalized and absolute amount of mutual information between the current and "Companion" images. The normalized value is a measure of image similarity that is suitable for images of similar intensity different types [39, 40].

A method is proposed and verified to select the optimal segmentation of stack reconstruction for 5D short-axis cuts as well as the cuts of the original MRI flow according to an accuracy selection criterion of the watershed segmentation. To make this selection, a precision comparison parameter has been defined. This is the value of mutual information between the images acquired from the sample and the projections of the segmented volumes. In this work, it has been shown that this mutual information parameter between the segmented volume and the reference volume is correlated.

To estimate the difference between acquired images and segmented volumes, an MI coefficient was used. MI proved to be an effective discrepancy measure for comparing images and was even used for the registration of medical images. Higher MI values indicate a greater reduction in uncertainty (high correspondence between images) and a value of 0 means that the variables (images) are statistically independent. MI is given by [41].

$$MI = \Sigma_{a,b}\ P_{AB}(a,\ b)\log[P_{AB}(a,\ b)\ /\ P_A(a)P_B(b)] \quad (3)$$

On note par P_A (a), P_B (b) les histogrammes marginaux normalisés des images A et B, respectivement, P_{AB} (a, b) est leur histogramme commun, et a et b l'intensité valeurs d'une paire de voxels dans les images A et B.

4.3. Evaluation of the ejection fraction by topographic watershed segmentation: optimization with the maximization of mutual information

Our method is based on the watershed algorithm is the application of shape primitives. This watershed approach is applied to pixel groups based on their intensities in the 5D short-axis image. The output of the stack segmentation generated by these sequences represents the homogeneous areas of gray level intensities for each pixel representation. After applying this segmentation approach, the optimization is done with MI to

Table 4. Summary report.

Mesures	Estimate by the active contour approach (short-axis cut)			Clinical assessment (short-axis cut)		
	Healthy patient	Patient with genetic disease	Patient with heart failure	Healthy patient	Patient with genetic disease	Patient with heart failure
M-ED(g)	129	209	131	137	357,1	127,4
M-ES(g)	93	-49	151	147	366,4	141,4
EDV (ml)	109	269	194	126,2	135,3	131,9
ESV(ml)	50	50	108	41,1	17,1	61,1
SV(ml)	59	219	86	85,1	118,3	70,9
EF (%)	54	81	45	67,4	87,4	53,7
HR (bmp)	59	56	69	73	56	69
	Estimation par l'approche de contour (séquence du flux sanguin)/valve aortique			Not defined		
Mesures/Flow (925 ms)	Patient with genetic disease	Healthy patient	Patient with heart failure			
F-Net (ml)	0,314	Without flow study	0,106			
Vel (l-min)	0,192		0,00722			
F-asen (ml)	0,315		0,106			
F-des (ml)	-0,00105		0			
F-Reg (%)	0,0335		0			
	Estimation par l'approche de contour (séquence du flux sanguin)/valve mitral					
Mesures/Flow (852 ms)	Patient with genetic disease	Patient sain	Patient with heart failure			
F-Net (ml)	0,29	Without flow study	-0,0476			
Vel (l-min)	0,0117		-0,00324			
F-Asen (ml)	0,29		0,00343			
F-desc (ml	-0,000721		-0,051			
F-Reg (%)	0,248		1,49 e+03			
	Segmentation by watershed by topological distance	Healthy patient	Segmentation with watershed by topological distance	Clinical assessment		
	Patient with genetic disease	Without flow study	Patient with heart failure	Patient with genetic disease	Healthy patient Without flow study	Patient with heart failure
Mesures	Short-axis 5D cuts		Short-axis 5D cuts			
FE/S (%)	[85–91] diastole et systole step		[45–65] diastole and systole step	71		45
FE/V (%)	73,65		56,19	ND		ND
Mesures	Flow sequences 4D		Flow sequences 4D	ND		
F-regur (%)	0.19458	ND	0.39049			

evaluate the ejection fraction in the regions that contains our reconstruction and section stacks (5D minor axis and blood flow).

The measurement of the surface fraction of the selected pixels in the current image (short-axis 5D and blood flow sequence) is to count all the selected pixels and divide the number by either the total number of pixels in the image or by the total number of selected pixels in a selected memory image. On the other hand, the measurement of the volume fraction of the pixels selected in the reconstruction counts all the selected pixels and divides the number by the total number of pixels in the reconstruction of our models.

We present the design of our container in Figure 11 to manage our implementation process of the topological distance watershed approach as well as a description of our data format.

4.3.1. For 5D short-axis cuts: implementation and extraction of measurements

In order to implement the watershed, approach we chose a patient with a suspicion of having a genetic disorder. A comparison between the original image of the short-axis cut 5D and the segmented image was simulated as well as the estimate of the ejection fraction at the surface during the systole and diastole phase and a volume ejection fraction deduced with watershed = 73.65% in Figure 12.

A second case was selected in our database with suspicion of heart failure. A comparison between the original image of the short-axis cut 5D and the segmented image was simulated as well as the estimate of the ejection fraction at the surface during the systole and diastole phase and a volume ejection fraction deduced with watershed = 56.19%.

4.3.2. For 4D stream stacks: implementing and retrieving metrics

By adopting the same strategy for these two patients, we chose to segment the aortic port for the left side of the heart in the 4D stream stacks with a metric of the mutual information and the comparison was made with the function of two-point correlation in Figure 13.

The results shown in Table 3 support the effectiveness of choosing the watershed approach for the quantification and estimation of the fraction of regurgitation for aortic flow. Based on the "SPIN" imaging concept or "pixel velocity" imagery for the study of flow sequences, scaling and stack manipulation highlights the crucial moment between the change of the diastole phase and systole. This methodology aims to set the pixel speed at this critical instantiation and clarify the contour of cardiac morphology for blood flow cuts. This functional dimension of the flux is considered as fifth dimension f (t) for the flow cuts after the treatment that has been performed on the stacks in our container and with elimination of the morphological structure of the heart in 3D. This strategy was developed in the previous chapter to extract the fifth dimension in a reciprocal way for short-axis cuts by existing pixels around the myocardium for the deformation of the flow.

5. Discussion

In this section, a comparative summary in Table 4 between the active contour segmentation approach was described, its disadvantages compared to that presented in the clinical routine in short-axis sections and flow sequences. The results show that if we repeat the same contour segmentation approach we obtain for a healthy patient 13.4% tolerance rate for the estimation of the stroke fraction, 6.4% tolerance rate for a patient with genetic disease, 8.7% error rate for a patient with heart failure symptom. The impact of using the watershed approach by topographic distance shows an efficiency when estimating the ejection fraction for short axis 5D cuts as well as the regurgitation fraction for flow stacks; the results show that the regurgitation fraction by the contour approach for a patient case with symptom of the presence of a genetic disease is 0.0335% for an aortic valve, 0.248% for a mitral valve, an error rate 0.16% for estimating this parameter for the aortic orifice with the watershed segmentation approach. In return, for a patient with suspected heart failure (stenosis or regurgitation) the regurgitation fraction is estimated by 0% for aortic valve, 1.49 e $^{+03}$% for a mitral valve, an error rate 11.76% compared to the watershed segmentation approach. The results are validated clinically. The estimation of this crucial parameter for the medical decision for these two cases with the watershed approach is closer and more reasonable compared to the clinical assessment with high precision rate for evaluation of ejection fraction and regurgitation.

For medical decision making, it is concluded that the results seem to be promoters for the detection of cardiac abnormalities. The extraction of the fifth dimension of flow which consists in exiting the pixels around the myocardium makes it possible to avoid misalignment during the segmentation phase. According to Oliver tree vignaux [34], a delineation error of 20° can produce an error of 6% and this can have a huge impact on the estimation of the systolic ejection fraction. Following these observations, we have proposed to adopt the concept 5D imaging and changing the contour segmentation approach used in clinical routine to the watershed approach, and estimating the gray-gray pixel average at the myocardium to calculate the ejection fraction.

5.1. Model limitation

Detection of myocardial contours is an essential prerequisite for the detection and quantification of myocardial infarction and valve disease artificially induced in rats on cardiac MRIs with injection of contrast product.

We propose a method of segmentation by watershed on short axis cine fiesta slices of the left ventricle on cardiac MRIs and their study of flow. The gradient vector flux which has been proposed as the fifth dimension has enabled us to determine a fairly efficient method of detecting myocardial contours, despite noisy and low contrast images according to the acquisition criteria of cardiac examinations. Therefore, this method is not initialization dependent; the initial contour does not need to be very close to the desired contour. The segmentation is carried out in two stages: detection of the endocardium then detection of the epicardium from the endocardial contour previously obtained. Indeed, this segmentation approach based on 5D imaging requires performant machines with a parallel calculation with architecture (CPU-GPU) as well as powerful algorithms from Navies-Stokes to extract new measurements for medical diagnosis such as strain, stress and vortex field. The results to segmented contours was compared with the Report-CARD tool and we obtain encouraging results despite the limitations of our models.

6. Conclusion

The region-based segmentation approach of CAs allowing segmentation of the object of interest that benefits from the advantages of local and global statistics to guide the CA towards the contours of the object of interest was described. The proposed approach shows robustness both in for heterogeneous attributes with improper initialization of CA and in the criterion of noise in the image. Among the advantages of the contour segmentation approach is that topology changes are automatically handled. The distance function ϕ is used to manage stable and accurate numerical schemes while the geometric features of the contour can be assessed from the function ϕ. The formulation can be easily extended to larger dimensions. This method has an important computational cost, it consists of avoiding the calculations that on a band surrounding the zero level of ϕ and to update this band each time the curve approaches its edges. Thus, the calculation costs are significantly reduced. The main contribution, via this approach, is the estimation of the cardiac measurements for 4D short-axis sections and 2D blood flow sequences directly from the MRI, it is to mark the inaccuracy of these parameters for the same approach used in the clinical routine. Based on the definition and algorithms of watershed, we proposed an alternative solution for left ventricular myocardial segmentation in cine-type MRIs for 5D slices to evaluate ejection fraction and regurgitation fraction to evaluate the degree of severity of the leak in the aortic valve. The method has been validated clinically. We have shown the accuracy of the results produced

by watershed by comparing them with CA segmentation versus clinical routine. Finally, we presented an analysis indicating that the watershed applied globally to the space-time 5D space with the functional flow dimension makes it possible to maintain a certain regularity with respect to the experts' diagnosis.

The limit of this approach is the toughness of assessing the fraction of stenosis from the flow sequences, we then propose to model the aorta in 3D and solve the Navier-Stokes equation as a function of time for the blood fluids as perspective and extension of our strategy. For future works and prospects, artificial intelligence (AI) can boast great performance, particularly in image analysis for diagnostic purposes, but, in daily clinical practice, the results of AI are based on evidence. are still few in number, but expanding rapidly in cardiology. Thus, we propose to develop an approach of segmentation by contour and by supervised watershed based on deep learning to improve the accuracy of measurements for medical decision making.

7. Summary points

- Propose a comparative study between the contouring and topographic watershed segmentation approach for cardiac short-axis 5D sequences with MRI for medical decision.
- Analyze the fifth dimension which described as the excitation of pixels based on the gray scale around the myocardium without consideration of the morphological structure of the heart 3D (x,y,z) and the fourth dimension (time).
- apply an optimization of the topographic watershed approach with mutual information and extract a set of measurements (ejection fraction, regurgitation rate) within the left ventricle for three patient types (healthy, genetic pathology and heart failure).
- The results are considered interesting compared to the clinical assessment.
- The limit of this approach is the difficulty of estimating the fraction of stenosis from the flow sequences, we then propose to model the aorta in 3D and solve the Navier-Stokes equation as a function of time for the blood fluids as perspective and extension of our work.

Declarations

Author contribution statement

H. Sakly, M. Said and M. Tagina: Conceived and designed the experiments; Performed the experiments; Analyzed and interpreted the data; Contributed reagents, materials, analysis tools or data; Wrote the paper.

Funding statement

This research did not receive any specific grant from funding agencies in the public, commercial, or not-for-profit sectors.

Declaration of interests statement

The authors declare no conflict of interest.

Additional information

No additional information is available for this paper.

Acknowledgements

Many thanks to the Radiology and Medical Imaging Unit within the International Center Carthage Medical that supported this work and to the medical staff for providing us with an access to the patients' archive and the administrative framework for the warm welcome in their team.

References

[1] W. Zhao, X. Xu, Y. Zhu, F. Xu, Active contour model based on local and global Gaussian fitting energy for medical image segmentation, Optik 158 (2018) 1160–1169.
[2] Y.-C. Lin, C.-Y. Cheng, Y.-W. Cheng, C.-T. Shih, Skull repair using active contour models, Procedia Manuf 11 (2017) 2164–2169.
[3] Y. Chen, X. Yue, R.Y.D. Xu, H. Fujita, Region scalable active contour model with global constraint, Knowl.-Based Syst. 120 (2017) 57–73.
[4] J. Liu, L. Li, L. Wang, Acetowhite region segmentation in uterine cervix images using a registered ratio image, Comput. Biol. Med. 93 (2018) 47–55.
[5] P. Chondro, C.-Y. Yao, S.-J. Ruan, L.-C. Chien, Low order adaptive region growing for lung segmentation on plain chest radiographs, Neurocomputing 275 (2018) 1002–1011.
[6] P. Parida, N. Bhoi, Wavelet based transition region extraction for image segmentation, Future Comput. Inform. J. 2 (2017) 65–78.
[7] C. Liu, M.K.-P. Ng, T. Zeng, Weighted variational model for selective image segmentation with application to medical images, Pattern Recogn. 76 (2018) 367–379.
[8] C. Gout, C.L. Guyader, L. Vese, Segmentation under geometrical conditions using geodesic active contours and interpolation using level set methods, Numer. Algorithm. 39 (2005) 155–173.
[9] N. Badshah, K. Chen, Image selective segmentation under geometrical constraints using an active contour approach, Commun. Comput. Phys. (2009).
[10] L. Rada, K. Chen, A new variational model with dual level set functions for selective segmentation, Commun. Comput. Phys. 12 (2012) 261–283.
[11] J. Peng, F. Dong, Y. Chen, D. Kong, A region-appearance-based adaptive variational model for 3D liver segmentation, Med. Phys. 41 (2014), 043502.
[12] L. Mabood, H. Ali, N. Badshah, K. Chen, G.A. Khan, Active contours textural and inhomogeneous object extraction, Pattern Recogn. 55 (2016) 87–99.
[13] S. Derivaux, G. Forestier, C. Wemmert, S. Lefèvre, Supervised image segmentation using watershed transform, fuzzy classification and evolutionary computation, Pattern Recogn. Lett. 31 (2010) 2364–2374.
[14] M. Hammoudeh, R. Newman, Information extraction from sensor networks using the Watershed transform algorithm, Inf. Fusion 22 (2015) 39–49.
[15] M. Ciecholewski, Automated coronal hole segmentation from Solar EUV Images using the watershed transform, J. Vis. Commun. Image Represent. 33 (2015) 203–218.
[16] D. Kruk, A. Boucher, A. Lalande, A. Cochet, T. Sliwa, Segmentation integrating watershed and shape priors applied to cardiac delayed enhancement MR images, IRBM 38 (2017) 224–227.
[17] Z. Huang, S. Jiang, Z. Yang, Y. Ding, W. Wang, Y. Yu, Automatic multi-organ segmentation of prostate magnetic resonance images using watershed and nonsubsampled contourlet transform, Biomed. Signal Process Contr. 25 (2016) 53–61.
[18] A. Das, D. Ghoshal, Human skin region segmentation based on chrominance component using modified watershed algorithm, Procedia Comput. Sci. 89 (2016) 856–863.
[19] A.A. Kiaei, H. Khotanlou, Segmentation of medical images using mean value guided contour, Med. Image Anal. 40 (2017) 111–132.
[20] F. Duane, M.C. Aznar, F. Bartlett, D.J. Cutter, S.C. Darby, R. Jagsi, E.L. Lorenzen, O. McArdle, P. McGale, S. Myerson, K. Rahimi, S. Vivekanandan, S. Warren, C.W. Taylor, A cardiac contouring atlas for radiotherapy, Radiother. Oncol. J. Eur. Soc. Ther. Radiol. Oncol. 122 (2017) 416–422.
[21] S.J.W. Kim, S. Seo, H.S. Kim, D.-Y. Kim, K.W. Kang, J.-J. Min, J.S. Lee, Multi-atlas cardiac PET segmentation, Phys. Medica PM Int. J. Devoted Appl. Phys. Med. Biol. Off. J. Ital. Assoc. Biomed. Phys. AIFB. 58 (2019) 32–39.
[22] M. Lorenzo-Valdés, G.I. Sanchez-Ortiz, A.G. Elkington, R.H. Mohiaddin, D. Rueckert, Segmentation of 4D cardiac MR images using a probabilistic atlas and the EM algorithm, Med. Image Anal. 8 (2004) 255–265.
[23] Y. Wang, Y. Zhang, W. Xuan, E. Kao, P. Cao, B. Tian, K. Ordovas, D. Saloner, J. Liu, Fully automatic segmentation of 4D MRI for cardiac functional measurements, Med. Phys. 46 (2019) 180–189.
[24] M. Bustamante, S. Petersson, J. Eriksson, U. Alehagen, P. Dyverfeldt, C.-J. Carlhäll, T. Ebbers, Atlas-based analysis of 4D flow CMR: automated vessel segmentation and flow quantification, J. Cardiovasc. Magn. Reson. Off. J. Soc. Cardiovasc. Magn. Reson. 17 (2015) 87.
[25] A. Cristoforetti, L. Faes, F. Ravelli, M. Centonze, M. Del Greco, R. Antolini, G. Nollo, Isolation of the left atrial surface from cardiac multi-detector CT images based on marker controlled watershed segmentation, Med. Eng. Phys. 30 (2008) 48–58.
[26] J. Cousty, L. Najman, M. Couprie, S. Clément-Guinaudeau, T. Goissen, J. Garot, Segmentation of 4D cardiac MRI: automated method based on spatio-temporal watershed cuts, Image Vis Comput. 28 (2010) 1229–1243.
[27] H. Sakly, R. Mahmoudi, M. Akil, M. Said, M. Tagina, Moving towards a 5D cardiac model, J. Flow Visual. Image Process. 26 (2019).
[28] H. Sakly, M. Said, S. Radhouane, M. Tagina, Medical decision making for 5D cardiac model: template matching technique and simulation of the fifth dimension, Comput. Methods Progr. Biomed. 191 (2020) 105382.
[29] H. Sakly, M. Said, M. Tagina, Reconstruction of 5D cardiac MRI through the blood flow registration: simulation of the fifth dimension and assessment of the left ventricular ejection fraction, Netw. Model. Anal. Health Inform. Bioinforma. 9 (2020) 61.
[30] S. Osher, R. Fedkiw, Level Set Methods and Dynamic Implicit Surfaces, Springer-Verlag, New York, 2003. www.springer.com/gp/book/9780387954820. (Accessed 12 April 2018).

[31] Y.H. Tsai, S. Osher, Level set methods in image science, Proc. 2003 Int. Conf. Image Process. Cat 3 (2003) 631–634. No03CH37429.
[32] W.A. Fares, Détection et suivi d'objets par vision fondés sur segmentation par contour actif basé région, phdthesis, Université Paul Sabatier - Toulouse III, 2013 (accessed April 5, 2018), https://tel.archives-ouvertes.fr/tel-00932263/document.
[33] D. Adalsteinsson, J.A. Sethian, A fast level set method for propagating interfaces, J. Comput. Phys. 118 (1995) 269–277.
[34] O. Vignaux, Imagerie cardiaque : scanner et IRM, second ed., ELSEVIER MASSON, 2011 (accessed April 11, 2017), https://www.elsevier-masson.fr/imagerie-cardiaque-scanner-et-irm-9782294712258.html.
[35] F. Meyer, Topographic distance and watershed lines, Signal Process. 38 (1994) 113–125.
[36] J.B.T.M. Roerdink, A. Meijster, The watershed transform: definitions, algorithms and parallelization strategies, Fundam. Inf. 41 (2000) 187–228.
[37] L. Najman, M. Schmitt, Watershed of a continuous function, Signal Process. 38 (1994) 99–112.
[38] J. Cousty, Lignes de partage des eaux discrètes : théorie et application à la segmentation d'images cardiaques, phdthesis, Université de Marne la Vallée, 2007. https://tel.archives-ouvertes.fr/tel-00321885/document. (Accessed 3 April 2018).
[39] J.P.W. Pluim, J.B.A. Maintz, M.A. Viergever, Image registration by maximization of combined mutual information and gradient information, in: Med. Image Comput. Comput.-Assist. Interv. – MICCAI 2000, Springer, Berlin, Heidelberg, 2000, pp. 452–461.
[40] D. Mattes, D.R. Haynor, H. Vesselle, T.K. Lewellyn, W. Eubank, Nonrigid multimodality image registration, in: Med. Imaging 2001 Image Process, International Society for Optics and Photonics, 2001, pp. 1609–1621.
[41] A. Okariz, T. Guraya, M. Iturrondobeitia, J. Ibarretxe, A parameter for the assessment of the segmentation of TEM tomography reconstructed volumes based on mutual information, Micron 103 (2017) 64–77.